

ANALYSIS OF STATIC ANGLE OF REPOSE WITH RESPECT TO POWDER MATERIAL PROPERTIES

OLIVER MACHO^{a,*}, KARIN DEMKOVÁ^b, ĽUDMILA GABRIŠOVÁ^a,
MATÚŠ ČIERNY^a, JITKA MUŽÍKOVÁ^c, PAULÍNA GALBAVÁ^d, ŽOFIA NIŽNANSKÁ^d,
JAROSLAV BLÁŠKO^d, PETER PECIAR^a, ROMAN FEKETE^a, MARIÁN PECIAR^a

^a Slovak University of Technology in Bratislava, Faculty of Mechanical Engineering, Institute of Process Engineering, Námetie Slobody 17, 812 31 Bratislava, Slovakia

^b High School of Jur Hronec, Novohradská 3, 821 09 Bratislava, Slovakia

^c Charles University, Faculty of Pharmacy, Department of Pharmaceutical Technology, Ak. Heyrovského 1203, 500 05 Hradec Králové, Czech Republic

^d Comenius University in Bratislava, Faculty of Natural Sciences, Institute of Chemistry, Ilkovičova 6 - Mlynská dolina, 842 15 Bratislava, Slovakia

* corresponding author: oliver.macho@stuba.sk

ABSTRACT. This paper investigates the Angle of Repose (*AoR*) of powder materials with respect to their morphological and rheological properties. Glass beads, sand, flour and semolina of different particle sizes were used as the experimental materials. The investigated material was analysed with respect to particle shape and size. The rheological properties of the material were obtained by a shear cell test. The *AoR* was analysed in terms of cohesion, bulk density, particle size and circularity. More cohesive materials such as the flour samples exhibited the largest *AoR* > 40°, indicating their poor flowability. Glass bead samples with a high circularity value had significantly lower *AoR* than the flour. The Angle of Internal Friction values were not dependent on those of the *AoR*. Using a dimensional analysis, a mathematical model was developed to determine the *AoR* values based on the material properties. By the application of this model, highly accurate calculation of the value of *AoR* is made possible.

KEYWORDS: Angle of repose, cohesion, powders, angle of internal friction, bulk density.

1. INTRODUCTION

Investigation of the flow properties of powder or granular materials is a key area for the correct design of equipment working with such material types. Powder flowability means the capacity of a powder to flow under a specified set of conditions [1]. There are several techniques to determine flowability. However, a single reliable and widely applicable method of measuring of flowability does not exist, because of the variety of both powder materials and the influence of handling on the measurement results [2]. One of the methods for quickly determining the nature of this flow is the measurement of the Angle of Repose (*AoR*). The *AoR* measurement is used in many applications of processing, storing and handling powder materials, determining the slope stability, furnace design and many other uses. Physically, the *AoR* can be defined as the angle that differentiates the transitions between phases of a granular material. One of the most commonly used definitions of the *AoR* is the steepest slope of an unconfined material, measured from the horizontal plane on which the material can be heaped without collapsing [3]. This angle is also sometimes referred to as the critical slope angle or friction angle. Measuring the *AoR* has a wide area of application, ranging from pharmaceutical through chemical, agricultural,

mining engineering and geology to civil engineering uses [4]. The two basic types of the *AoR* are static and dynamic [5]. The static *AoR* is determined by using an experimental apparatus with a funnel-defined geometry through which the experimental material is poured. The falling material is collected on a defined circular pad under the funnel (fixed-base) or is loosely poured onto a plate (free-base) with the individual layers of material forming a steep pile (cone) [6]. The dynamic angle is determined by a rotating drum in which the material under investigation is reformed by the effect of rotation as by an avalanche. By measuring the slope of the moving powder from the center of the experimental station, we obtain the Avalanche Angle [7]. Among modern trends in the measurement of the *AoR* are the following techniques: 3D scanning of created piles [8, 9], or modeling by the discrete element method [10–12]. Flow properties of powders present a complex characteristic of a bulk powder, and they are affected by physico-chemical and mechanical properties of the particles [13]. The interaction forces of the powder consist of Van der Waals forces, capillary forces, electrostatic forces of the powders, and similar [14]. Moreover, the size, shape and material surface elasticity are also dominant factors. Several authors have devoted their *AoR* research to materials



FIGURE 1. Scheme of measurement of AoR (Fine glass bead particles).

with different material properties, such as aluminum powder [15], corn grains, lignite, wood chips [16], asphalt concrete [17], rice and flours [18], pulverized coal [19], iron ore [20], biomass [21], sugar [22] or fine dust from power plants [23]. The aim of this study was to analyse the impact of rheological and morphological properties of selected materials and their effect on the AoR size. In this paper, we investigated the static AoR obtained from measurements on an experimental station using the fixed-base method. Using dimensional analysis, a mathematical model was developed to determine the AoR values based on the material properties of the experimental samples. By an application of this model, it is possible to calculate the value of static AoR with a high accuracy.

2. MATERIAL AND METHODS

2.1. EXPERIMENTAL MATERIAL

Two types of sand and semolina with different particle sizes were used as experimental coarse-grained materials. The sand was delivered in size intervals, coarse (1.0 – 1.6 mm) and finer (0.8 – 1.2 mm). Another material samples were five types of glass beads, from fine to approximately 0.5 mm in size. Cohesive materials were represented by flour with different fractions (Strong, Soft flour). The bulk density (BD) of the material was determined by means of a measuring cylinder into which 100 ml of material was loaded. The BD value was determined from a known sample volume and weight, with the experiments repeated three times.

2.2. MEASUREMENT OF ANGLE OF REPOSE

The Static AoR measurement ran in an accordance with European Pharmacopoeia 9.0 (2.9.36) according to ASTM recommendations (C1444-00). The experimental material was poured through a funnel of diameter $D = 10$ mm onto a pad of diameter $d = 50$ mm until a cone was formed which did not change shape with a continued pouring. The excess material fell over the edge of the pad. Static AoR measurements were performed 3 times for each material. AoR values were obtained by the analysis of individual measurements (Fig. 1) and calculated according to the relationship (1).

$$AoR = \arctan \left[\frac{H}{d/2} \right] \quad (1)$$

where H is the height of the cone and d is the diameter of the pad.

2.3. MORPHOLOGY OF EXPERIMENTAL POWDRES

The size and shape of the particles were analysed using a Morphologi G3 (Malvern) optical microscope. Samples of the material were evaluated based on the volume of the individual particles. The characteristic particle size marker was the median of Circle Equivalent (CE). CE represents the diameter of a circular particle with the same volume as the particle under the investigation. The particle shape was evaluated using Circularity Φ . The higher the value, the more circular the particles examined: $\Phi = 1$ corresponds perfectly to circular particles.

2.4. POWDERS RHEOLOGY

Using a FT4 (Freeman Technology) powder rheometer based on ASTM-D6773-16 [24], individual samples were analysed from the rheological point of view. Using the Shear Cell Test (sample consolidation 9 kPa), the cohesion (c) and the angle of internal friction (AIF) were determined. The experiments were repeated three times for each material. The pre-shear value was 9 kPa and the shear head produced normal stresses of 7, 6, 5, 4 and 3 kPa in the materials, and the corresponding shear stresses were recorded for the individual values of the normal stresses. From the normal and shear stress points a yield locus was created. The Angle of internal friction is the tangent of the linearized yield locus [25]. The higher the AIF value, the smaller the interparticular forces, and the more flowable the powder. Cohesion represents the degree of coherence of the test substance. Its value is influenced by interparticle forces (van der Waals), material moisture, particle size and others. The more cohesive the material, the worse flow properties and lower the ff_c flow function parameter [26].

2.5. EVOLUTION OF ANGLE OF REPOSE IN TIME

The increase of the AoR over time was determined by an image analysis of the videos captured by a tripod-mounted Nikon D5500 digital camera. The created videos were transformed into static images representing defined times of the pouring. ImageJ software was used to analyse the pile growth over time [27]. The dimensions and shape of the piles were then transformed from pixels to centimeters using a scale. In these experiments, semolina was used as the experimental material. Shape and pile size were examined by pouring the material onto a horizontal base from a height of 14 cm depending on different pouring times. The material was poured through 5 and 8 mm diameter drain holes of funnels.

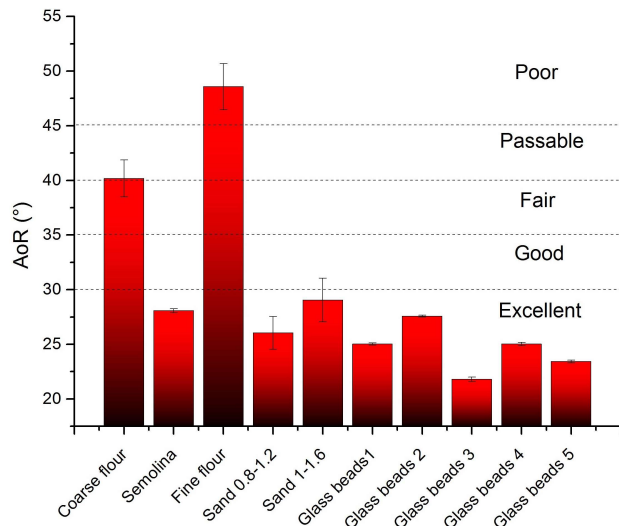


FIGURE 2. Values of AoR for different experimental material.

3. RESULTS AND DISCUSSION

3.1. ANGLE OF REPOSE

Fig. 2 shows the values of the AoR . Based on the values of the AoR , the flow properties of the examined material can be established [28]. The graph shows the highest value of the AoR was found with soft flour $AoR = 48.58 \pm 2.1^\circ$. This value corresponds to poor flow properties. The second worst flow properties were observed in strong flour $AoR = 40.18 \pm 1.7^\circ$, on the border of passable and fair flow properties. Semolina and glass beads, materials with the largest particles, have excellent flow properties based on the AoR ($AoR < 30^\circ$). Experimental data can be found in Tab. 1.

3.2. PARTICLE MORPHOLOGY AND BULK DENSITY

Individual material properties were analysed based on their effect on the AoR value. Coarse sand had lower AoR values than fine flour particles (Fig. 3). The median particle size values of the coarse and fine sand were $CE = 1459 \mu\text{m}$ and $CE = 1044 \mu\text{m}$ respectively. For glass beads of increasing CE values, the AoR decreased with the exception of glass beads 4. The finer flour has a bigger AoR than strong flour. For sand materials, a greater value was observed for sand of the interval 1 – 1.6 mm.

The circularity value (Fig. 4) was higher for sand particles ranging between 0.8 – 1.2 mm ($\Phi = 0.96$) than for the sand particles between 1 – 1.6 mm ($\Phi = 0.88$). On the base of this finding, it could be said that the smaller particles with higher Φ have better flow properties than the particles with a higher CE . Similar examples are shown in study [29] with mannitol particles. Sphericity values decreased minimally as the size of the glass beads increased. All circular glass bead particles of $\Phi > 0.99$ featured an

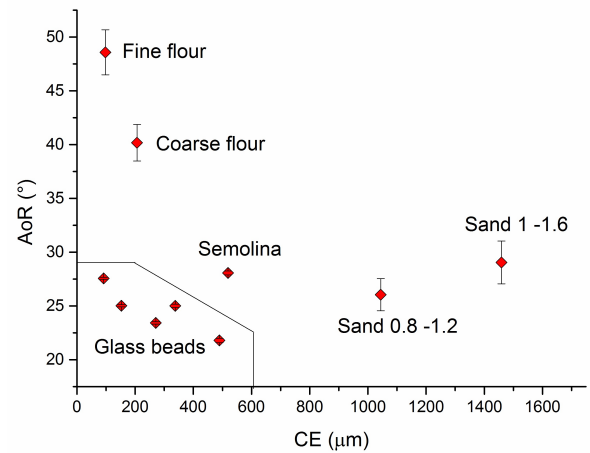


FIGURE 3. Influence of particle size (CE) on AoR .

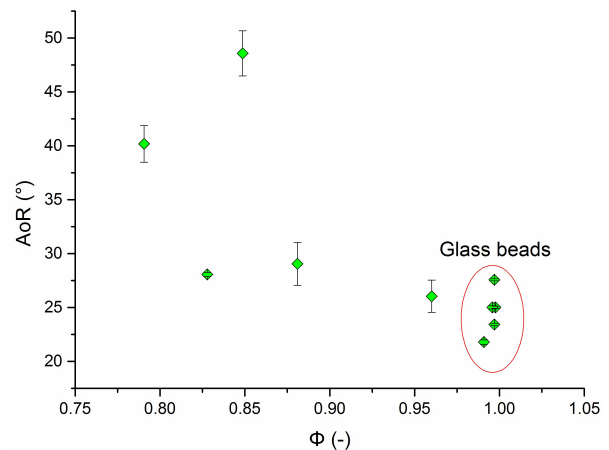


FIGURE 4. Influence of circularity (Φ) on AoR .

AoR value of $24 \pm 3^\circ$, for all size fractions. Strong flour particles had the lowest value of circularity ($\Phi = 0.79$).

3.3. EVALUATION OF BULK DENSITY

Bulk densities of the samples were $BD > 1400 \text{ kg}\cdot\text{m}^{-3}$ for most materials (Fig. 5), with the maximum value of standard deviations being $0.02 \text{ kg}\cdot\text{m}^{-3}$. The sand particles in the 0.8 – 1.2 range had the highest value of bulk density $1.63 \pm 0.02 \text{ kg}\cdot\text{m}^{-3}$ and the soft flour particles had the lowest bulk density ($0.632 \pm 0.003 \text{ kg}\cdot\text{m}^{-3}$). The dynamic effect of falling particles of materials with higher BD values impacting on the substrate did not allow the formation of stiff cones on the pad. Due to the fact that self-weight particles tends to roll over an existing heap, move away and reach a stable state far away from the point of the fall. Except for semolina, samples with a lower BD value had values of the AoR higher than 40° . Semolina particles had a significantly larger particle size of $CE = 519.3 \mu\text{m}$ compared to flour samples.

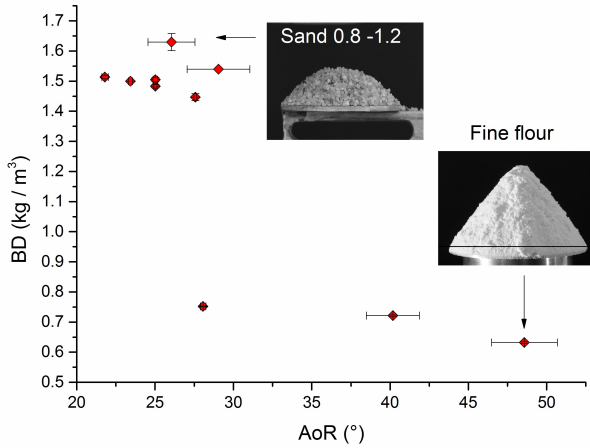


FIGURE 5. Influence of bulk density (BD) on AoR .

3.4. EVALUATION OF PARTICLE RHEOLOGY

The parameters describing the flowability of the powder can be determined from the yield locus. In order to measure the course of yield locus, several of the tests must be performed, where the specimens must first be consolidated at identical normal stress, preshear. Then, the specimens are sheared to failure, under different normal stresses. The yield locus follows from a plotted curve through all measured shear points. In Fig. 6, a graph of the Shear Cell Test from the FT4 rheometer for sands, flours and semolina is presented. Sand particles have a significantly steeper trend, which means they also have higher AIF values. Significant deviations in the individual experiments were observed with the flour particles. The glass beads had values of $AIF < 26^\circ$ in all cases. Fig. 7 shows the graph from the Shear Cell Test of glass beads. If the glass beads have a higher CE , then the yield locus line is significantly steeper, which implies a higher AIF value. With an increasing glass bead particle size, the value of AIF increased proportionally. For experiments with the glass bead particles significantly smaller deviations were observed.

From the cohesion impact on the AoR graph (Fig. 8), materials with a higher value of cohesion and, at the same time, the smallest AIF achieved the highest AoR values. The trend of the graph confirms the assumption that the greater the influence of interparticle forces, expressed by means of cohesion, the more coherent is the material, allowing the formation of a steeper pile. The most cohesive were the soft flour particles, where $c=1.597\pm 0.23$ kPa. For the glass bead particles, the value of cohesion for all types of the material was $c<0.25$ kPa. The measurement of the cohesion confirmed that it had a significant effect on the flow properties of the examined materials, as well as the AoR size.

Based on the graph (Fig. 9), it is possible to say that there is no direct relationship between the AoR with load-free materials and the AIF angle, which expresses the friction between the particles when an

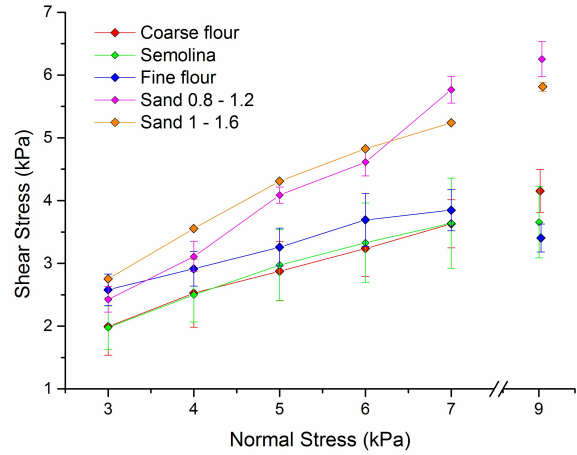


FIGURE 6. Shear Cell Test of sands, flours and semolina.

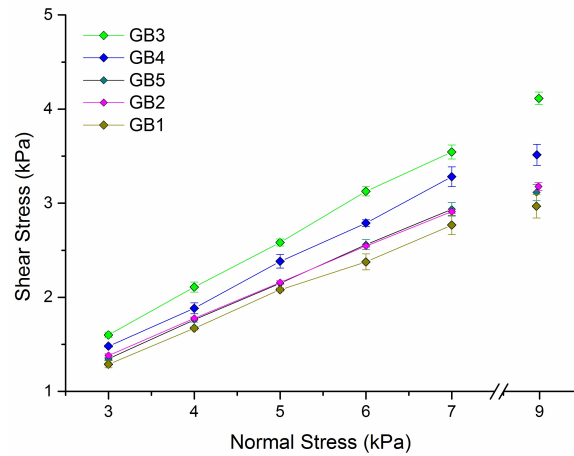


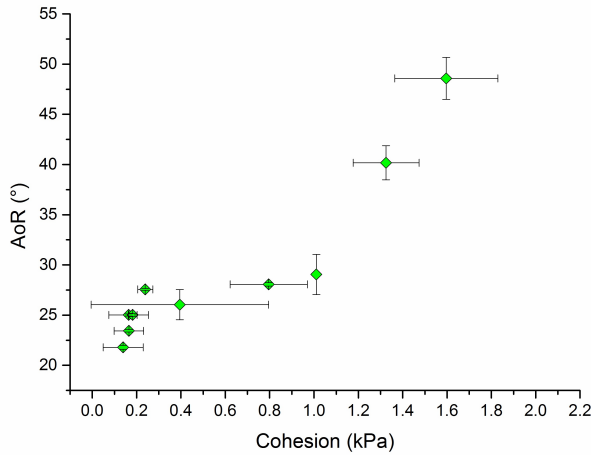
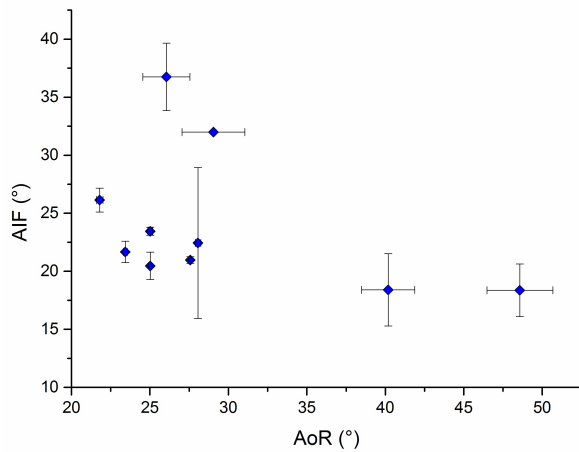
FIGURE 7. Shear Cell Test of glass beads particles.

external load is applied. A similar finding was published in a paper [4]. For flour samples, the AIF was on average 20° lower than the AoR , while the sand samples had a higher AIF value. The AIF values for glass beads were accompanied by minor deviations. The highest value of AIF was found for 0.8 – 1.2 mm sand, $AIF = 36.75 \pm 2.9^\circ$.

Fig. 10 shows a graphical dependence between cohesion and the ff_c flow function parameter. The graph shows that these two parameters are power dependent. As shown by the higher cohesion value, the flow properties of the powder materials, whether expressed by AoR or ff_c , are impaired.

3.5. AOR IN TIME

In Fig. 11, 12, graphical dependences of the growth of the pile when the semolina was poured onto a horizontal base from a height of 14 cm is shown. On the basis of the Beverloo equation, the discharge velocity of the semolina particles was calculated, for a funnel with a 5 mm outlet being 0.002081 g/s and for an 8 mm outlet funnel being 0.007134 g/s. For an 8 mm funnel,

FIGURE 8. Influence of cohesion (c) on AoR .FIGURE 9. Comparison between Angle of Internal friction (AIF) and AoR .

due to its larger cross-sectional area and therefore higher discharge speed, the flow time of the material was shorter. In both cases, the final shape of the pile began to form after 13 s. At a lower discharge velocity, the pile reached a height of 4.86 cm, and at a higher velocity, it reached a height of 4.65 cm. The higher discharge velocity caused that the dynamic effect of a larger amount of falling particles did not allow the formation of a higher pile. Particles falling at higher discharge velocities tend to roll over existing heap.

3.6. MODEL DESCRIPTION

The dimensional analysis method was chosen to create the AoR related model and the material properties obtained from the experiments. In relation (2), the same quantity ($^{\circ}$) is present on both sides. The values of the individual material properties used for modeling were obtained as average values from repeating measurements.

$$AoR = \frac{c \cdot \Phi \cdot AIF}{CE \cdot g \cdot BD} \quad (2)$$

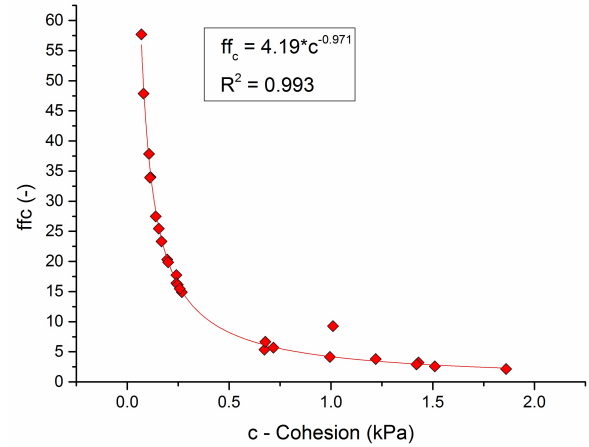
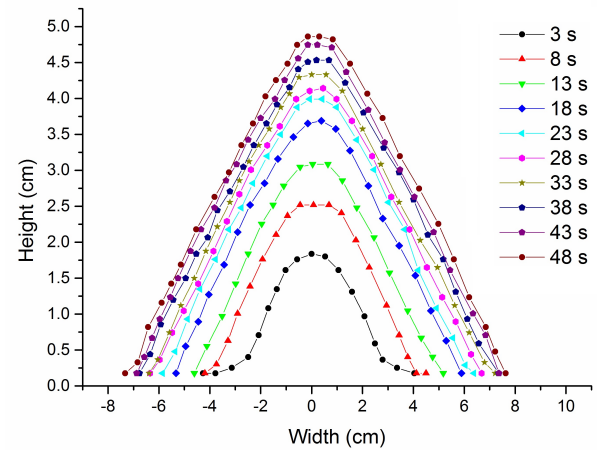


FIGURE 10. Influence of cohesion on flow function parameter.

FIGURE 11. Evolution of AoR during tests with 5 mm funnel.

where AoR ($^{\circ}$) is the angle of repose, c is cohesion (Pa), Φ is the particle circularity ($-$), CE is the equivalent particle diameter (m), g - gravitational acceleration ($m \cdot s^{-2}$), BD bulk density ($kg \cdot m^{-3}$), AIF angle of internal friction ($^{\circ}$).

In Fig. 13, a dependence between the AoR and the established criterion from the right side of the equation (2) is shown. A power mathematical model based on the experimental data describing the relationship between the AoR and material properties was developed using a non-linear regression (3). The coefficient of determination was $R^2 = 0.92$. The differences between the AoR values calculated according to the model created and the AoR values from the experiment are found in Fig. 14. Based on the model, the AoR value for samples of the studied materials with a standard deviation $STDEV=1.95^{\circ}$ can be calculated. This value is sufficient to correctly characterize the flow of the experimental material.

Sample	CE (μm)	Φ (-)	AOR ($^\circ$) \pm st. dev	AIF ($^\circ$) \pm st. dev	c (kPa) \pm st. dev	BD ($\text{kg}\cdot\text{m}^{-3}$) \pm st. dev
Strong flour	206.2	0.791	40.18 ± 1.70	18.40 ± 3.11	1.325 ± 0.148	0.722 ± 0.002
Semolina	519.3	0.828	28.07 ± 0.18	22.43 ± 6.49	0.796 ± 0.174	0.725 ± 0.001
Soft flour	97.7	0.849	48.58 ± 2.10	18.37 ± 2.26	1.597 ± 0.232	0.632 ± 0.002
Sand 0.8-1.2	1044	0.960	26.05 ± 1.50	36.75 ± 2.90	0.395 ± 0.400	1.630 ± 0.028
Sand 1.0-1.6	1459	0.881	29.05 ± 2.00	32.00 ± 0.00	1.010 ± 0.000	1.540 ± 0.000
GB1	152.5	0.998	25.02 ± 0.10	20.47 ± 1.18	0.164 ± 0.089	1.483 ± 0.005
GB2	91.71	0.997	27.57 ± 0.09	20.97 ± 0.28	0.239 ± 0.034	1.447 ± 0.011
GB3	489.6	0.991	21.80 ± 0.20	26.13 ± 1.02	0.139 ± 0.090	1.513 ± 0.006
GB4	338.0	0.996	25.02 ± 0.15	23.45 ± 0.35	0.182 ± 0.019	1.505 ± 0.007
GB5	271.0	0.997	23.43 ± 0.12	21.67 ± 0.92	0.165 ± 0.067	1.500 ± 0.000

TABLE 1. Properties of experimental samples (Values of AoR , AIF , c and BD are averaged from three measurements $n=3$).

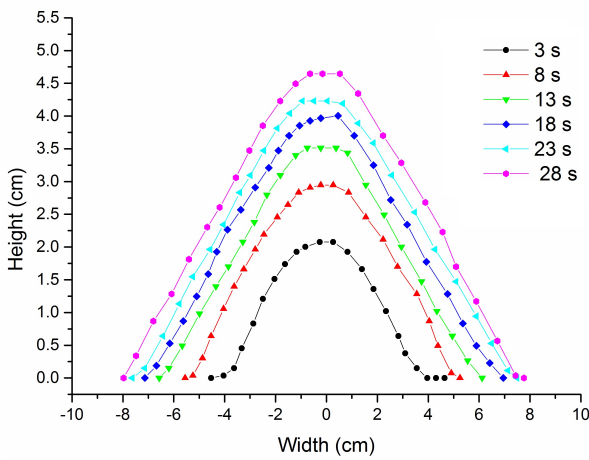


FIGURE 12. Evolution of AoR during tests with 8 mm funnel.

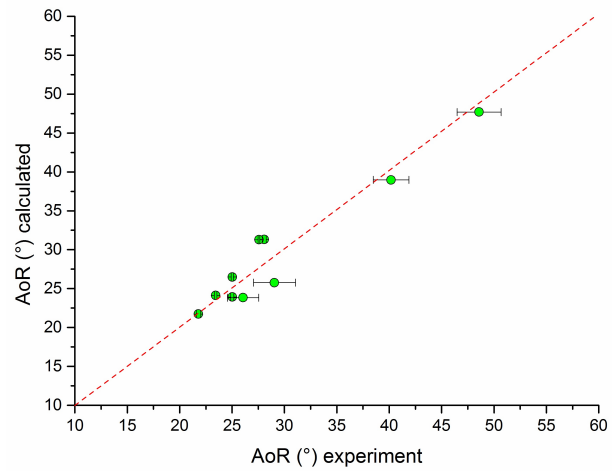


FIGURE 14. Differences between calculated and experimental AoR .

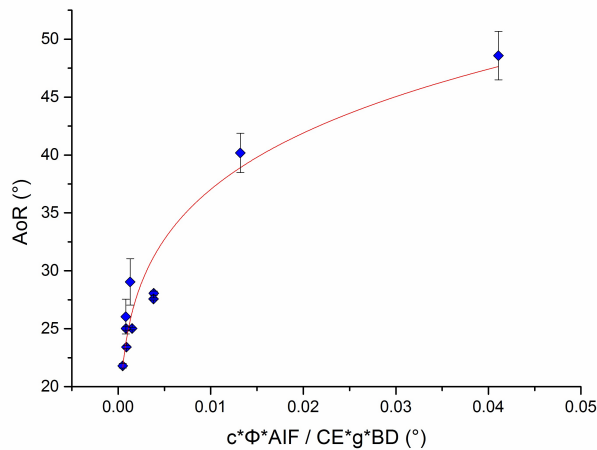


FIGURE 13. Relationship between AoR and created criteria.

$$AoR = 84.19 \cdot \left(\frac{c \cdot \Phi \cdot AIF}{CE \cdot g \cdot BD} \right)^{0.178} \quad (3)$$

4. CONCLUSION

In this paper, we examined the AoR and its relation to the morphological and rheological properties of the experimental material. The analysed properties of the material had a significant impact on the AoR . The highest AoR values were achieved with cohesive flour samples. The AoR increased with increasing cohesion. Spherical particles of glass beads with high BD values had the lowest AoR values, which confirmed their good flow properties. Similarly, larger particles of sand and semolina also had good flow properties. Using the Shear Cell Test, we obtained AIF values that did not show a direct relationship to the AoR . The dependence between the cohesion and material flow properties was found. It has been shown that the discharge rate has an influence on the size and shape of the formed pile. Using a dimensional analysis, a mathematical model was developed to determine the AoR based on the properties of the experimental material. Based on this model, it is possible to determine an AoR value with a standard deviation of

1.95°, which makes it possible to reliably characterize the flow properties of the experimental material.

LIST OF SYMBOLS

c	Cohesion [Pa]
d	Diameter of the pad [m]
ff_c	Flow function parameter [–]
g	Gravitational acceleration [m s^{-2}]
AoR	Angle of repose [°]
AIF	Angle of internal friction [°]
BD	Bulk density [kg m^{-3}]
CE	Equivalent particle diameter [m]
H	Height of the cone [m]
Φ	Particle circularity [–]

ACKNOWLEDGEMENTS

The authors would like to thank Mr. John Peter Blight for language correction.

This article was created with the support of the Ministry of Education, Science, Research and Sport of the Slovak Republic within the Research and Development Operational Programme for the project “University Science Park of STU Bratislava”, ITMS 26240220084, co-funded by the European Regional Development Fund.

This work was supported by the Slovak Research and Development Agency under contract No. APVV-18-0348.

The authors wish to acknowledge the Ministry of Education, Science, Research and Sport of the Slovak Republic for the financial support of this research by grant KEGA 016STU-4/2019.

REFERENCES

- [1] G. Xu, P. Lu, M. Li, et al. Investigation on characterization of powder flowability using different testing methods. *Experimental Thermal and Fluid Science* **92**(November 2017):390–401, 2018. DOI:10.1016/j.expthermflusci.2017.11.008.
- [2] Z. Zatloukal, Z. Šklubalová. Drained angle of free-flowable powders. *Particulate Science and Technology* **26**(6):595–607, 2008. DOI:10.1080/02726350802501369.
- [3] A. Mehta, G. C. Barker. The dynamics of sand, 1994. DOI:10.1088/0034-4885/57/4/002.
- [4] H. M. Beakawi Al-Hashemi, O. S. Baghabra Al-Amoudi. A review on the angle of repose of granular materials. *Powder Technology* **330**:397–417, 2018. DOI:10.1016/j.powtec.2018.02.003.
- [5] D. Geldart, E. Abdullah, A. Hassanpour, et al. Characterization of powder flowability using measurement of angle of repose. *China Particuology* **4**(3-4):104–107, 2006. DOI:10.1016/s1672-2515(07)60247-4.
- [6] H. Hurychová, P. Ondrejček, Z. Šklubalová, et al. The influence of stevia on the flow, shear and compression behavior of sorbitol, a pharmaceutical excipient for direct compression. *Pharmaceutical Development and Technology* **23**(2):125–131, 2018. DOI:10.1080/10837450.2017.1315132.
- [7] H. Hurychová, M. Kuentz, Z. Šklubalová. Fractal Aspects of Static and Dynamic Flow Properties of Pharmaceutical Excipients. *Journal of Pharmaceutical Innovation* (iii), 2017. DOI:10.1007/s12247-017-9302-0.
- [8] A. Wójcik, P. Klapa, B. Mitka, I. Piech. The use of TLS and UAV methods for measurement of the repose angle of granular materials in terrain conditions. *Measurement: Journal of the International Measurement Confederation* **146**:780–791, 2019. DOI:10.1016/j.measurement.2019.07.015.
- [9] A. Wójcik, P. Klapa, B. Mitka, J. Śladek. The use of the photogrammetric method for measurement of the repose angle of granular materials. *Measurement: Journal of the International Measurement Confederation* **115**(July 2017):19–26, 2018. DOI:10.1016/j.measurement.2017.10.005.
- [10] T. Roessler, A. Katterfeld. Scaling of the angle of repose test and its influence on the calibration of DEM parameters using upscaled particles. *Powder Technology* **330**:58–66, 2018. DOI:10.1016/j.powtec.2018.01.044.
- [11] V. Hassanzadeh, C. M. Wensrich, R. Moreno-Atanasio. Elucidation of the role of cohesion in the macroscopic behaviour of coarse particulate systems using DEM. *Powder Technology* 2019. DOI:10.1016/j.powtec.2019.07.070.
- [12] T. Roessler, A. Katterfeld. DEM parameter calibration of cohesive bulk materials using a simple angle of repose test. *Particuology* **45**:105–115, 2019. DOI:10.1016/j.partic.2018.08.005.
- [13] Ž. Trpělková, H. Hurychová, P. Ondrejček, et al. Predicting the Angle of Internal Friction from Simple Dynamic Consolidation Using Lactose Grades as Model. *Journal of Pharmaceutical Innovation* 2019. DOI:10.1007/s12247-019-09387-3.
- [14] Z. Guo, X. Chen, H. Liu, et al. Theoretical and experimental investigation on angle of repose of biomass-coal blends. *Fuel* **116**:131–139, 2014. DOI:10.1016/j.fuel.2013.07.098.
- [15] M. M. De Campos, M. D. C. Ferreira. A comparative analysis of the flow properties between two alumina-based dry powders. *Advances in Materials Science and Engineering* **2013**(December 2013), 2013. DOI:10.1155/2013/519846.
- [16] M. Rackl, F. E. Grötsch, M. Rusch, J. Fottner. Qualitative and quantitative assessment of 3D-scanned bulk solid heap data. *Powder Technology* **321**:105–118, 2017. DOI:10.1016/j.powtec.2017.08.009.
- [17] A. K. Swamy, V. Matolia, G. V. Ramana. Use of angle of repose of aggregates as an indicator of asphalt concrete properties. *Construction and Building Materials* **168**:849–857, 2018. DOI:10.1016/j.conbuildmat.2018.02.091.
- [18] G. Lumay, F. Boschini, K. Traina, et al. Measuring the flowing properties of powders and grains. *Powder Technology* **224**:19–27, 2012. DOI:10.1016/j.powtec.2012.02.015.
- [19] W. Wang, J. Zhang, S. Yang, et al. Experimental study on the angle of repose of pulverized coal. *Particuology* **8**(5):482–485, 2010. DOI:10.1016/j.partic.2010.07.008.
- [20] H. Wei, X. Tang, Y. Ge, et al. Numerical and experimental studies of the effect of iron ore particle shape on repose angle and porosity of a heap. *Powder Technology* 2019. DOI:10.1016/j.powtec.2019.05.031.

- [21] G. Xu, M. Li, P. Lu. Experimental investigation on flow properties of different biomass and torrefied biomass powders. *Biomass and Bioenergy* **122**(July 2018):63–75, 2019. DOI:10.1016/j.biombioe.2019.01.016.
- [22] L. C. dos Santos, R. Condotta, M. d. C. Ferreira. Flow properties of coarse and fine sugar powders. *Journal of Food Process Engineering* 2018. DOI:10.1111/jfpe.12648.
- [23] C. Lanzerstorfer. Dusts from dry off-gas cleaning: comparison of flowability determined by angle of repose and with shear cells. *Granular Matter* 2017. DOI:10.1007/s10035-017-0745-2.
- [24] H. Shi, R. Mohanty, S. Chakravarty, et al. Effect of particle size and cohesion on powder yielding and flow. *KONA Powder and Particle Journal* **2018**(35):226–250, 2018. DOI:10.14356/kona.2018014.
- [25] J. Zegzulka, D. Gelnar, L. Jezerska, et al. Internal friction angle of metal powders. *Metals* 2018. DOI:10.3390/met8040255.
- [26] M. Alshafiee, W. H. AlAlaween, D. Markl, et al. A predictive integrated framework based on the radial basis function for the modelling of the flow of pharmaceutical powders. *International Journal of Pharmaceutics* 2019. DOI:10.1016/j.ijpharm.2019.118542.
- [27] F. Fulchini, U. Zafar, C. Hare, et al. Relationship between surface area coverage of flow-aids and flowability of cohesive particles. *Powder Technology* 2017. DOI:10.1016/j.powtec.2017.09.013.
- [28] M. Šimek, V. Grünwaldová, B. Kratochvíl. Comparison of compression and material properties of differently shaped and sized paracetamols. *KONA Powder and Particle Journal* 2017. DOI:10.14356/kona.2017003.
- [29] Y. Takeuchi, T. Tomita, J. Kuroda, et al. Characterization of mannitol granules and powder: A comparative study using two flowability testers. *International Journal of Pharmaceutics* **547**(1-2):106–113, 2018. DOI:10.1016/j.ijpharm.2018.05.061.